

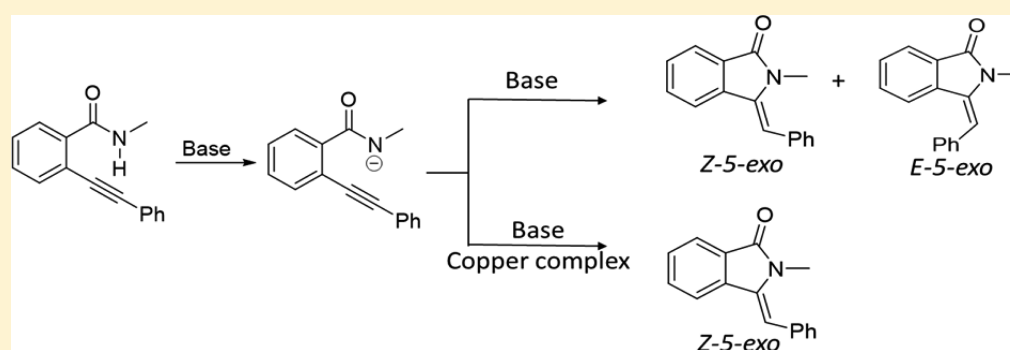
# 3-Methyleneisoindolin-1-one Assembly via Base- and CuI/L-Proline-Catalyzed Domino Reaction: Mechanism of Regioselective Anionic Cyclization

Li Li<sup>†,§</sup> and Benjamin G. Janesko<sup>\*,‡</sup>

<sup>†</sup>Shimadzu Institute for Research Technology, University of Texas at Arlington, Arlington, Texas 76019, United States

<sup>‡</sup>Department of Chemistry and Biochemistry, Texas Christian University, Fort Worth, Texas 76129, United States

**S** Supporting Information



**ABSTRACT:** Anionic cyclization of *o*-alkynylbenzamides is proposed as a crucial step in many heterocycle syntheses. The cyclization can produce three products: *Z*-3-methyleneisoindolin-1-one (*Z*-5-*exo*), *E*-3-methyleneisoindolin-1-one (*E*-5-*exo*), and isoquinolinone (6-*endo*). Under base catalysis, the selectivity is generally poor. However, a copper-involved domino reaction of coupling and cyclization gives surprising selectivity for the thermodynamically disfavored *Z*-5-*exo* product (*Org. Lett.* **2009**, *11*, 1309–1312). We study the selectivity of anionic cyclization in the presence of  $K_2CO_3$  and copper-*L*-proline, using surveys of the experimental literature and density functional theory (DFT) calculations. The *o*-alkynylbenzamide is predicted to be readily deprotonated by many bases, with subsequent cyclization via nucleophilic attack of the amide  $N^-$  to alkyne. In the absence of copper, *endo-exo* selectivity is predicted to arise from substituent effects, while *Z/E* selectivity is a sensitive function of the tautomerization rate of an alkenyl anion intermediate. Most importantly, we predict that the remarkable selectivity of the copper-involved reaction occurs because copper-*L*-proline “locks” the alkene anion intermediates into the initially formed *Z*-5-*exo* configuration. Calculations on other metals suggest that soft Lewis acid additives provide a potential route to improved regiocontrol of other anionic cyclizations.

## INTRODUCTION

Nucleophilic cyclization between an amide and an alkyne is an efficient way of producing heterocycles in high yield. This method has been used to synthesize a variety of important heterocycles, including the biologically interesting alkaloids cepharone B<sup>1</sup> and lennoxamine,<sup>2</sup> and the medically interesting compounds 5-(2-acylethynyl)uracil and 1,3-dihydro-3-(2-hydroxy-2-methylpropyl)-2*H*-isoindol-1-one<sup>3</sup> among many others.<sup>4,5</sup> These reactions demonstrate good regio- and stereospecificity in the cyclized product.

There are two main categories of catalysts reported for *o*-alkynylbenzamide intramolecular cyclization: bases and copper complexes. Strong bases such as NaOEt<sup>3</sup> and *t*-BuOK<sup>6</sup> often produce a mixture of *Z*-5-*exo* and *E*-5-*exo* isoindolinones and 6-*endo* isoquinolinones. Mild bases such as TBAF can also produce mixtures of *Z*-5-*exo* and *E*-5-*exo* isoindolinones.<sup>5</sup> The selectivity of base-catalyzed cyclization is a sensitive function of substituents,<sup>3</sup> and base alone does not provide high selectivity.

However, a recent copper-catalyzed domino coupling of 2-halobenzamides and terminal alkynes was reported to almost exclusively provide *Z*-5-*exo* indolinone products.<sup>7</sup> Subsequent copper(II)-catalyzed domino couplings also reported *Z*-5-*exo* products.<sup>2,8</sup> Cyclization of *N*-alkoxy-*ortho*-alkynylbenzamides in the presence of stoichiometric  $CuCl_2/NCS$  selectively provided 5-*exo-dig* products.<sup>9</sup> *o*-Alkynylbenzamide cyclization with ammonium acetate to form 1-aminoisoquinolones is accelerated by Au(III) catalysts.<sup>10</sup>

The initial steps of these copper-involved domino reactions involve production of *o*-alkynylbenzamide intermediates, which can be isolated at short reaction times.<sup>8</sup> The metal-mediated cross-couplings producing these intermediates are well studied.<sup>11</sup> However, the roles of the base, copper, and ligand in the subsequent *o*-alkynylbenzamide cyclization calls for a

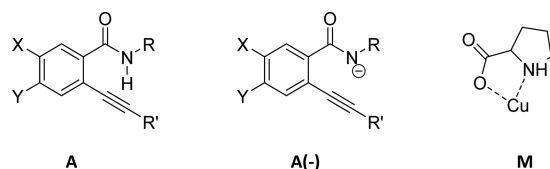
Received: August 4, 2016

Published: November 3, 2016

better understanding, especially in regard to the surprising regioselectivity. Experimental groups have suggested that the copper–ligand complex (or electrophile) attaches to the alkyne and potentially controls the regiochemistry.<sup>1,2,8,9</sup> However, no detailed theoretical examination has been reported.

In this paper, we report a computational mechanistic study of the cyclization of *o*-alkynylbenzamide **A**, in the presence of  $K_2CO_3$  and copper(I)-L-proline catalyst **M** (Scheme 1). We

**Scheme 1. Reactant A, Anionic Intermediate A(–), and Model Copper(I)–Proline Catalyst M**



address several questions about this anionic cyclization. (a) Can the weak base  $K_2CO_3$  alone deprotonate molecule **A** to intermediate **A(–)**? (b) What controls the selectivity of **A(–)** cyclization in the absence of copper? (c) Where does copper bind to molecule **A**? (d) Does copper make it easier for  $K_2CO_3$  to deprotonate **A**? (e) How does copper change the selectivity of **A(–)** cyclization and accelerate the overall reaction? (f) Why do certain substituents yield mixtures of *Z*-5-*exo* and *E*-5-*exo* products? (g) Could metals other than copper give similar effects? Our answers to these questions suggest new experimental routes to improved regiocontrol of these widely used reactions.

We begin by reviewing the experimental literature on the selectivity of intramolecular anionic cyclization of *o*-alkynylbenzamides. Kundu and Khan reported that derivatives of **A** produced in palladium-catalyzed cross-coupling were cyclized by added  $NaOEt$ . While most derivatives yielded 5-*exo* cyclization, aliphatic alkynes ( $R' = alkyl$ ) gave appreciable 6-*endo* product.<sup>3</sup> Deng Yuan Li and co-workers reported *t*-BuOK catalyzed cyclization of alkynoyls, alkynylamines, and alkynylbenzamides, with *o*-alkynylbenzamide cyclization at 80 °C selectively producing *E*-5-*exo* product.<sup>6</sup> Vasilievsky and co-workers presented a detailed experimental and computational study of *o*-acetylnyl benzoic acid hydrazide cyclization ( $R = NH_2$ ), concluding that 6-*exo* products are thermodynamically stable and kinetically preferred when  $R' = alkyl$ .<sup>4</sup> This contrasts with the *Z*-5-*exo* products reported in copper-involved domino reactions.<sup>8,9</sup> Bubar and co-workers found that cyclization of **A** in the presence of TBAF yielded *Z/E* mixtures whose composition strongly depended on  $R'$ , reporting selective *Z*-5-*exo* product formation with  $R' = 4-(TIPSC\equiv C)C_6H_4$ .<sup>5</sup>

Because our simulations are based on ref 8, we here introduce that study in more detail.  $CuI/L$ -proline with a variety of bases ( $K_2CO_3$ ,  $K_3PO_4$ ,  $Cs_2CO_3$ ) and solvents (isopropanol, DMF, DMSO) catalyzed formation of 3-methyleneisindolin-1-ones from 2-bromobenzamides and phenylacetylene. *o*-Alkynylbenzamide **A** could be isolated if the reaction time was shortened. Most reactions produced only *Z*-5-*exo* product under the reaction conditions: aryl bromide (0.5 mmol), 1-alkyne (0.75 mmol),  $CuI$  (0.05 mmol), *L*-proline (0.15 mmol), *i*-PrOH (1 mL), 85 °C. However,  $Y = NO_2$  carried out in solvents DMSO and *i*-PrOH both resulted in mixtures of *E*-5-*exo* and *Z*-5-*exo* isomers (*Z/E* = 5:1).  $R = Et_2N(CH_2)_2$  carried

out in DMF at 100 °C for the best product yield afforded mostly *E*-5-*exo* isomers (*Z/E* = 1:14).

## COMPUTATIONAL METHODS

We simulate anionic cyclization using density functional theory with the B3LYP hybrid exchange-correlation functional and the 6-31+G(d,p) basis set, using the Gaussian 09 suite of programs.<sup>12</sup> Solvation by 2-propanol or DMSO is simulated with the conductor-like screening model.<sup>13</sup> Calculations comparing different metals (Table 4) use the LANL2DZ basis set and effective core potential for all metals.<sup>14</sup> Reaction intermediates and transition states are confirmed to have zero and one imaginary frequencies in the vibrational Hessian. Transition states are confirmed to connect the intermediates of interest by displacing the geometry forward and backward along the imaginary mode, then reoptimizing to a local minimum. The Gibbs free energy in solution is taken as the total energy evaluated in continuum solvent, plus ideal-gas, rigid-rotor, and harmonic-oscillator thermal corrections evaluated at 298 K with continuum-solvent-optimized geometry and vibrational models. Or restated, the Gibbs free energy is simply taken as the “Sum of electronic thermal and Free Energies” printed by Gaussian 09 from a geometry optimization and vibrational frequency calculation in continuum solvent. This approach is discussed in ref 15.

Most calculations consider the substitution pattern  $X = Y = H$ ,  $R' = Ph$ , and  $R = Me$ . The  $R = Me$  group serves as a simple model for the  $R = benzyl$  of most experiments in ref 8. Deng Yuan Li and co-workers reported *t*-BuOK catalyzed cyclization of this specific molecule  $X = Y = H$ ,  $R' = Ph$ ,  $R = Me$  (referred to as molecule **3f** in that reference), reporting high yields of the *E*-5-*exo* cyclization product.<sup>6</sup> All energies are in kJ/mol. Supplementary tables, and computed geometries and energies of all species, are included as Supporting Information.

## RESULTS AND DISCUSSION

This section is organized as follows. Each subsection addresses one of the questions (a)–(g) posed in the Introduction. We begin with question (a), whether weak bases such as  $K_2CO_3$  can deprotonate **A**.

**a. Amide Deprotonation.** Previous experimental studies of base catalyzed cyclization propose that the cyclization of **A** starts with deprotonation.<sup>3–6,8</sup> Strong bases such as  $NaOEt$ <sup>3</sup> and *t*-BuOK<sup>6</sup> can clearly deprotonate the amide. *N*-deuterated benzamides dissolved with  $Cu(OAc)_2$  in *t*-AmylOH at 120 °C exhibited essentially complete H/D exchange, consistent with deprotonation by acetate.<sup>2</sup> Addition of water to TBAF in THF reduces the basicity of the fluoride ion and disfavors cyclization of **A** derivatives, consistent with rate-limiting deprotonation.<sup>5</sup> Cyclization of a related (2-ethynylphenyl)methanol species in DMSO gives yields of 94% with *t*-BuOK and 64% with  $K_2CO_3$ , suggesting it is deprotonated by both bases.<sup>6</sup> However, it is worth studying whether the weaker  $K_2CO_3$  base used in ref 8 can deprotonate **A** in the DMSO and isopropanol solvents used experimentally, or whether complex **M** is required for deprotonation.

Detailed simulations of deprotonation mechanisms are enormously challenging, and even calculation of the  $pK_a$  in organic solvent is demanding.<sup>16</sup> Accordingly, we approximate the  $pK_a$  of **A** and  $KHCO_3$  (the conjugate acid of  $K_2CO_3$ ) based on the  $pK_a$  measured in DMSO for closely related compounds phenol ( $pK_a(DMSO, 25\text{ °C}) = 18.0$ ),  $C_6H_5CONHNH_2$  ( $pK_a(DMSO, 25\text{ °C}) = 18.9$ ), and  $MeCONH_2$  ( $pK_a(DMSO, 25\text{ °C}) = 25.5$ ).<sup>17</sup> DFT calculations predict that proton transfer from  $KHCO_3$  to  $PhO(-)$  has  $\Delta G^\circ = 40\text{ kJ/mol}$  (7 pH units) in DMSO, giving a predicted  $KHCO_3$   $pK_a(DMSO, 25\text{ °C}) = 25$ . Similarly, DFT calculations predict that proton transfer from **A** to  $C_6H_5CON(-)NH_2$  has  $\Delta G^\circ = 27\text{ kJ/mol}$  (5 pH units) in

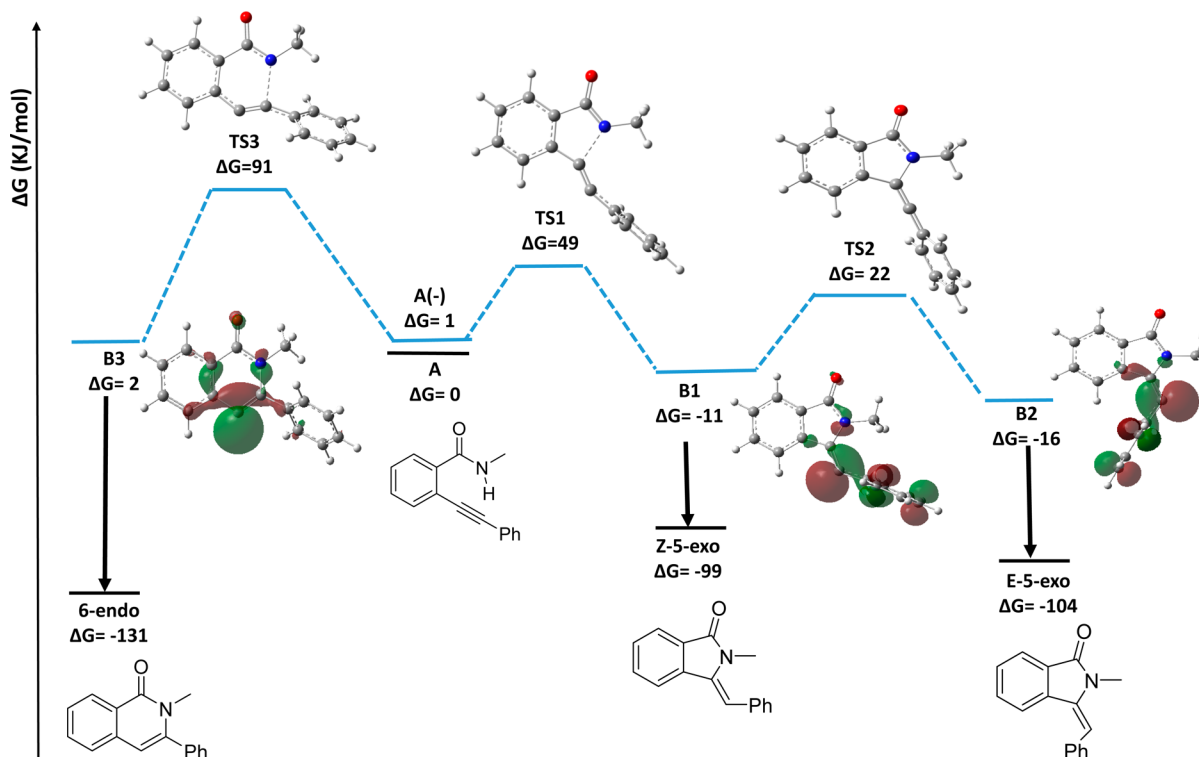


**Figure 1.** Computed Gibbs free energy surface for cyclization of deprotonated intermediate  $A(-)$  ( $R = \text{Me}$ ,  $R' = \text{Ph}$ ,  $Y = \text{H}$ ), leading to 6-endo or 5-exo products. The zero of free energy is  $A$  and  $\text{KCO}_3^-$  base. The figure includes the computed structure of transition state **TS1**, **TS2**, and **TS3** and the computed structure and HOMO of intermediates **B1**, **B2**, and **B3**.

DMSO, giving a predicted  $A$   $\text{p}K_a(\text{DMSO}, 25^\circ\text{C}) = 24$ . Proton transfer from  $A$  to  $\text{MeCONH}(-)$  has  $\Delta G^\circ = -7$  kJ/mol ( $-1$  pH units) in DMSO, confirming the predicted  $A$   $\text{p}K_a(\text{DMSO}, 25^\circ\text{C}) = 24$ . The predicted  $\text{p}K_a$  values of  $A$  and  $\text{KHCO}_3$  are within 1 pH unit of each other, consistent with modest yields of deprotonated intermediate. This is supported by the computed Gibbs free energy of the reaction  $A + \text{KCO}_3(-) \rightarrow A(-) + \text{KHCO}_3$  (reaction 1). This reaction is predicted to be nearly thermoneutral ( $\Delta G^\circ = 1$  kJ/mol) in 2-propanol and modestly uphill ( $\Delta G^\circ = 5$  kJ/mol) in DMSO.

We conclude that the copper complex **M**, while being essential for the initial C–C coupling forming **A**, might not be required for **A**'s subsequent cyclization. This raises the question of how **M** might be involved in the cyclization selectivity. To answer this, we must consider question (b), how the cyclization proceeds in the absence of **M**.

**b. Base-Catalyzed Cyclization.** In base catalyzed anionic cyclization of reactant **A**, after deprotonation of the amide nitrogen to form  $A(-)$ , the cyclization selectivity is known to be controlled by the nature of substitution on the newly formed “internal” nucleophile  $N(-)$ .<sup>4</sup> Experiments find that aliphatic alkynes ( $R' = \text{alkyl}$ ) tend to produce the 6-endo product, while aromatic alkynes can produce either *Z*-5-exo or *E*-5-exo products.<sup>3</sup> A previous theoretical study of hydrazides of *o*-acetylenyl pyrazolcarbonyl acids ( $R = \text{NH}_2$ ) found that the 6-endo products are thermodynamically stable, that cyclization of the anionic intermediate is nearly thermoneutral, and the 6-endo alkenyl anion intermediate **B3** is relatively unstable for aromatic alkynes  $R = \text{Ph}$ .<sup>4</sup>

Figure 1 shows our computed free energy surface for  $\text{K}_2\text{CO}_3$ -catalyzed cyclization of **A** to *E*-5-exo, *Z*-5-exo, and 6-endo products, as well as the computed HOMO of representative intermediates. Intermediate **A** (center) is deprotonated to form

$A(-)$ , which (as discussed above) is computed to be nearly thermoneutral in isopropanol.  $A(-)$  can cyclize to alkenyl anion intermediate **B1** or **B2** (right) leading to 5-exo products, or can cyclize to alkenyl anion intermediate **B3** (left) leading to the 6-endo product. Solid vertical arrows indicate protonation of an alkenyl anion by  $\text{KHCO}_3$ , the conjugate acid of base  $\text{K}_2\text{CO}_3$ , to form the final product.

We first consider 5-exo/6-endo selectivity. Figure 1 shows that, while the 6-endo product is the most thermodynamically stable, production of the corresponding alkenyl anion intermediate **B3** is kinetically and thermodynamically disfavored for  $R' = \text{Ph}$ . This prediction matches the experiments cited above, in which base-catalyzed cyclization yields 5-exo products when  $R = \text{aryl}$  and 6-endo products when  $R' = \text{alkyl}$ .

The intermediates' computed HOMO provide a simple explanation for this selectivity. In 5-exo cyclization (intermediates **B1** and **B2**), the  $\sigma$  alkenyl anion can delocalize onto the aromatic  $R'$  via conjugation with the out-of-plane  $\pi$ -system. However, in 6-endo cyclization intermediate **B3**, the alkenyl anion carbon is separated by an  $\text{sp}^2$  carbon from  $R'$ , and the  $\sigma$  lone pair cannot conjugate with the  $R'$   $\pi$ -system. This stabilization exhibit preference toward 5-exo cyclization. To confirm this, Table 1 shows the relative energies of intermediates **B1**, **B2**, **B3** with aryl vs alkyl -substituted alkynes.

**Table 1.** Computed Gibbs Free Energies for Conversion of **A** to Alkenyl Anion Intermediates<sup>a</sup>

Species	<i>Z</i> -5-exo ( <b>B1</b> )	<i>E</i> -5-exo ( <b>B2</b> )	6-endo ( <b>B3</b> )
$R' = \text{Ph}$	-11.3	-16.4	2.0
$R' = \text{Me}$	35.7	28.3	-4.6

<sup>a</sup>Calculations compare aromatic and aliphatic  $R'$ .

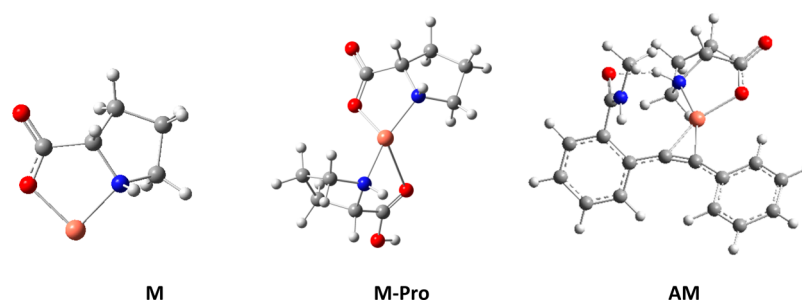


Figure 2. Computed geometries of model catalyst **M**, catalyst resting state **M-Pro**, and initial complex **AM**.

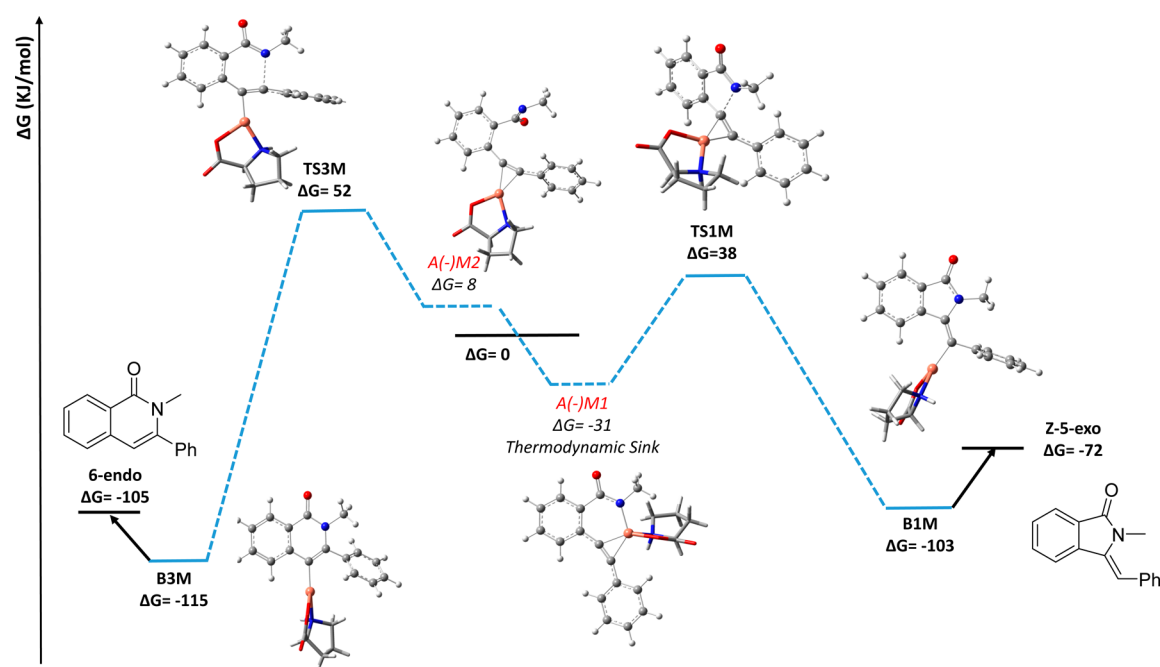


Figure 3. Computed Gibbs free energy surface for cyclization of deprotonated, metal-complexed intermediates **A(-)M1** and **A(-)M2** ( $R = \text{Me}$ ,  $R' = \text{Ph}$ ,  $Y = \text{H}$ ), leading to 6-endo and Z-5-exo products. The zero of free energy is **AM**,  $\text{KCO}_3(-)$  base, and free *L*-proline. The figure includes the computed structures of transition states **TS1M**, **TS3M** and intermediates **B1M**, **B3M**. Black arrows denote reprotonation by  $\text{KHCO}_3$ , and *L*-proline binding to the catalyst to recover the catalyst resting state **M-Pro**. To improve readability, the *L*-proline ligand is depicted as a wireframe structure.

The table confirms that the 6-endo intermediate is relatively stable for  $R' = \text{Me}$  and relatively unstable for  $R' = \text{Ph}$ , consistent with the calculations in ref 4.

We next consider *Z/E* selectivity in the 5-endo cyclizations. Recall that refs 3 and 6 showed that a strong base tends to give *Z/E* product mixtures, while ref 8 found that copper + a weak base generally yielded *Z*-5-exo products. Our explanation for this selectivity is based in part on a difference between our predicted mechanism for *o*-alkenylbenzamide cyclization and the predicted mechanisms for hydrazides ( $R = \text{NH}_2$ ) in ref 4. Unlike that study, we were unable to locate a transition state directly forming *E*-5-exo intermediate **B2** from deprotonated **A(-)**. The *E*-5-exo state in ref 4 was stabilized by an intramolecular hydrogen bond between  $R = \text{NH}_2$  and the forming alkenyl anion. Molecule **A(-)** lacks this stabilizing interaction. Instead, we predict that *Z*-5-exo intermediate **B1** can tautomerize to **B2** through allylic transition state **TS2**. The tautomerization barrier is substantially lower than the barrier to **B1** formation, and intermediates **B1** and **B2** are nearly isoenergetic. Our calculations thus predict that, in the absence of copper, the *Z/E* selectivity will be a sensitive function of the

relative rates at which intermediate **B1** is protonated, and the rate at which it tautomerizes to **B2**.

The mechanism in Figure 1 rationalizes many previous experiments. Comparing refs 3–6 suggests that, in the absence of the copper catalyst, the *Z/E* selectivity of the 5-endo cyclization is a very sensitive function of reaction conditions. Figure 1 suggests that this is due to the close competition between the rate of **B1** protonation, and the rate and equilibrium constant of its tautomerization to **B2**. Figure 1 also offers a hint to the selective *Z*-5-exo cyclization seen in ref 8: intermediate **B1** is the first to form, suggesting that trapping **B1** gives selective *Z*-5-exo cyclization. Comparison between the selective *Z*-5-exo cyclization in ref 8 and the widely varying *Z/E* ratios in refs 3–6 suggests that the copper coupling catalyst **M** likely plays a role in controlling cyclization selectivity.

We need to point out that all the calculations above treated solvent with a continuum model. However, in real experiments, the isopropanol solvent presumably can readily protonate intermediates **B1**–**B3**. This could potentially change the endo-exo selectivity. We have therefore re-evaluated the mechanisms in Figure 1, with a single explicit molecule of isopropanol hydrogen-bonded to the alkenyl anions. The 6-endo alkenyl

anion **B3** is dramatically stabilized by hydrogen bonding, with the product **B3-*i*PrOH** having essentially complete proton transfer from isopropanol to the 6-endo product. However, the predicted barrier to 6-endo cyclization is still substantially higher than the barriers to Z-5-exo cyclization or Z/E tautomerization. This confirms the overall picture of Figure 1. The Supporting Information provides details.

**c. Copper Catalyst M: Structure and Binding to A.** To understand how catalyst **M** could enhance the selectivity to Z-5-exo cyclization, we first consider its structure in solution and its binding to reactant **A**. We follow previous simulations of copper-catalyzed C–C coupling reactions<sup>12</sup> and model the active catalyst as neutral bidentate Cu(I)–L-proline complex **M**. We also follow previous simulations in considering a catalyst resting state **M-Pro**,<sup>12a,18</sup> where **M** coordinates a second neutral proline ligand. Figure 2 shows the computed structures of **M**, **M-Pro**, and the most stable complex between catalyst **M** and reactant **A**. Complex **AM** is a  $\pi$ -alkyne copper(I) complex similar to that proposed in the copper-cocatalyzed Sonogashira reaction.<sup>19</sup> Copper binding activates the alkyne, twisting the Ph–C $\equiv$ C bond angle from 180° in free **A** to 157° in **AM**.

We next consider the strength of the copper–alkyne interaction in **AM**. We find that molecule **A** can displace the second proline ligand from **M-Pro**. Displacement reaction **A** + **M-Pro**  $\rightarrow$  **AM** + L-proline (reaction 2) has a thermodynamically favorable predicted  $\Delta G^\circ = -27$  kJ/mol. The Supporting Information shows that other models for the catalyst resting state give qualitatively similar results. We conclude that the copper catalyst can bind and activate **A**.

**d. Copper Catalyst M: Amide Deprotonation.** Our results in section (a) suggest that K<sub>2</sub>CO<sub>3</sub> alone can deprotonate amide **A**, without assistance from copper. We next ask whether copper binding makes it easier to deprotonate the amide. We find that deprotonation of the initial complex **AM** gives two kinds of stable structures, exemplified by intermediates **A(-)M1** and **A(-)M2** in Figure 3. The first kind (**A(-)M1**) has copper bound to both the alkyne and the deprotonated nitrogen. The second kind (**A(-)M2**) has copper bound only to the alkyne. We also found several other isomers with copper bound only to the alkyne. All are nearly isoenergetic with **A(-)M2** and are included as Supporting Information.

We find that copper binding only to the alkyne does not make it easier to deprotonate the amide. Deprotonation of **AM** to **A(-)M2** by KCO<sub>3</sub>(-) gives a predicted  $\Delta G^\circ = 8$  kJ/mol, slightly less favorable than the  $\Delta G^\circ = 1$  kJ/mol needed to deprotonate **A** itself (cf. reaction 1). However, deprotonation of **AM** to **A(-)M1** gives  $\Delta G^\circ = -31$  kJ/mol, much more favorable than deprotonating **A** itself. Copper stabilizes the deprotonated form. We will show in the next section that **A(-)M1** is a thermodynamic sink whose copper–nitrogen bond must be rebroken in the cyclization. However, we will also suggest that **A(-)M1** is important for selectivity.

**e. Copper Catalyst Complex: Acceleration and Selectivity.** We are now in a position to address our main question: why does cyclization in the presence of copper yield such high selectivity for Z-5-exo products with a high yield? Figure 3 shows the computed Gibbs free energy surfaces for cyclizing **A(-)M1** and **A(-)M2**. We find that **A(-)M2** gives the 6-endo intermediate **B3M** through a high transition state **TS3M**. **A(-)M1** gives exclusively the Z-5-exo intermediate **B1M** through a lower transition state **TS1M**. Even though the copper–nitrogen bond in **A(-)M1** is a thermodynamic sink, the overall barrier to cyclization is still lower for Z-5-exo

cyclization. (Other isomers with copper bound only to alkyne can also cyclize to Z-5-exo intermediate **B1M**. The cyclization barriers are comparable to or somewhat above **TS1M**, but are below **TS3M**. These alternate pathways are discussed in the Supporting Information.)

Figure 3 provides an explanation for the Z-5-exo selectivity seen in the presence of copper(I)–L-proline. Recall from Figure 1 that, in the absence of copper, Z-5-exo intermediate **B1** can readily tautomerize to the corresponding E-5-exo intermediate **B2**. In contrast, Figure 3 shows that the product of anionic cyclization **B1M** has its alkenyl anion strongly stabilized by coordination to copper. Indeed, reprotonation to form the Z-5-exo product and the catalyst resting state is predicted to be thermodynamically uphill (black arrows). The copper “locks” the initial Z-5-exo intermediate **B1M** into place, preventing the Z–E tautomerization seen in the absence of copper. Reference 1 found similar results for *o*-alkynylbenzamide electrophilic cyclization by I<sub>2</sub>, with selective formation of the Z-5-exo product in which iodine remained bound to the exo carbon. (The Supporting Information presents one possible mechanism for reprotonation of **B1M** with retention of the Z-5-exo configuration. Reference 10 also proposes a related mechanism for copper displacement from an alkenyl anion intermediate with retention of configuration.) We conclude that this copper–carbon complex is central to the selectivity observed experimentally.

Figure 3 also shows that copper will modestly accelerate the overall reaction. Table 2 summarizes the rate-limiting barriers

**Table 2. Summary of the Rate-Limiting Barriers to Z-5-exo and 6-endo Formation (kJ/mol)**

catalyst	Z-5-exo	6-endo
base (Figure 1)	49	91
base and copper (Figure 3)	38	52

from Figures 1 and 3. Copper catalyst **M** lowers the overall barrier to forming the Z-5-exo intermediate, while giving a modest (and still acceptable) decrease in the difference between Z-5-exo and 6-endo barriers.

**f. E-5-exo Products from Certain Substituents.** Figures 1 and 3 help explain the intriguing substituent effects on selectivity reported in ref 8. That reference found that substituting molecule **A** with Y = NO<sub>2</sub> (cf. Scheme 1) gave a mixture of Z-5-exo and E-5-exo products, while substitutions Y = OMe and X = Cl gave exclusively the Z-5-exo product. We suggest this is because Y = NO<sub>2</sub> lowered the amide pK<sub>a</sub> enough to have cyclization catalyzed by base alone. Table 3 shows the pK<sub>a</sub>(DMSO, 25 °C) computed as in section (a) from proton

**Table 3. Computed pK<sub>a</sub> in DMSO, and Gibbs Free Energy for Deprotonation by KCO<sub>3</sub>(-), for Various Derivatives of A<sup>a</sup>**

substitution	pK <sub>a</sub> (DMSO, 25 °C)	$\Delta G^\circ$ for deprotonation by KCO <sub>3</sub> (-) (kJ/mol)	experimental product distribution
X = Y = H	24.3	1	Z-5-exo
Y = OMe	25.4	7	Z-5-exo
X = Cl	23.6	-3	Z-5-exo
Y = NO <sub>2</sub>	21.6	-16	E-Z mixture

<sup>a</sup>Results are compared to the experimental product distributions reported in ref 8.

transfer to MeCONH<sub>2</sub>, as well as Gibbs free energies for **A** deprotonation by KCO<sub>3</sub>(-) (reaction 1). Y = NO<sub>2</sub> significantly lowers the amide pK<sub>a</sub>, while the other substitution patterns do not substantially change the pK<sub>a</sub> relative to X = Y = H. This suggests that, under the experimental conditions of ref 8, at least some of the reactant (A, Y = NO<sub>2</sub>) will undergo base-catalyzed cyclization *without* bound copper. This leads to the mixture of *Z* and *E* isomers typically seen in base-catalyzed cyclization.<sup>2–6</sup> Substitution with a coordinating amine R = Et<sub>2</sub>N(CH<sub>2</sub>)<sub>2</sub> was also shown in ref 8 to give a *Z/E* mixture. We speculate that this may reduce the copper's ability to coordinate and stabilize the anionic intermediate **B1**.

**g. Other Metals.** Figures 1 and 3 also suggest a more general mechanism for regiocontrol of anionic cyclizations. The figures suggest that any species that binds to and protects the initially formed alkenyl anion intermediate **B1** could shift the selectivity toward *Z-5-exo* cyclization. We have conducted a preliminary study of several metals, by considering their relative binding affinities for intermediate **B1** vs carbonate base. We model the **B1** affinity of metal M(*n*+) as the reprotonation **B1**(-)-M(*n*+) + H<sub>2</sub>CO<sub>3</sub> → *Z-5-exo* + HCO<sub>3</sub>(-)-M(*n*+) (reaction 3). Less negative reaction energies correspond to greater stabilization of intermediate **B1**. Table 4 presents the

**Table 4. Computed Gibbs Free Energy (kJ/mol) for Reprotonation of **B1**–Metal Complexes by H<sub>2</sub>CO<sub>3</sub><sup>a</sup>**

M( <i>n</i> +)	Δ <i>G</i> <sup>o</sup> for reprotonation by H <sub>2</sub> CO <sub>3</sub> (kJ/mol)
Mg(2+)	-233
Ca(2+)	-252
Zn(2+)	-146
Cu(+)	-111
Ag(+)	-137
Au(+)	-5

<sup>a</sup>Less negative values indicate more stabilization of **B1** intermediate.

computed Gibbs free energies of reaction 3, evaluated for six bare metal cations Mg(2+), Ca(2+), Zn(2+), Cu(+), Ag(+), Au(+). The results suggest that hard Lewis acids such as Mg(2+) and Ca(2+) have a strong preference for base and will not effectively stabilize the soft alkenyl anion. In contrast, soft Lewis acids such as Au(+) effectively stabilize the alkenyl anion. Zn(2+) has an intermediate effect. The results motivate exploration of soft Lewis acids such as gold salts as additives in anionic cyclizations.

## CONCLUSION

The calculations presented in this work suggest answers to all of our questions about this reaction. (a) Weak bases such as K<sub>2</sub>CO<sub>3</sub> can deprotonate amide **A**, activating it for anionic cyclization. (b) Base-catalyzed cyclization preferentially yields *S-exo* products with R' = aryl, because the corresponding alkenyl anion intermediates **B1** and **B2** are stabilized by resonance. The *Z/E* selectivity of the *S-exo* cyclization is a sensitive function of the rates at which the initial intermediate **B1** is protonated to the *Z-5-exo* product, vs tautomerized to intermediate **B2**. (c) Copper(I) proline catalyst **M** can form a thermodynamically stable complex with the alkyne. (d) **M** does not aid deprotonation of **A**, save for potential formation of a thermodynamic sink A(-)M1. (e) **M** significantly improves the selectivity to *Z-5-exo* cyclization, by "locking" the anionic cyclization intermediate into its initially formed geometry **B1-M**. **M** provides overall lower rate-limiting barriers, increasing

the overall yield. (f) The mechanism presented here seems to rationalize the *E-5-exo* products formed with certain substitution patterns. (g) Soft Lewis acids such as Au(+) could provide a more general route to regiocontrol of anionic cyclizations, via stabilization of intermediate **B1**. We conclude that a greater mechanistic understanding of these reactions could provide useful practical results. This motivates further experimental study of the temperature and pH dependence of cyclization, and more detailed simulations.<sup>20</sup>

## ASSOCIATED CONTENT

### Supporting Information

The Supporting Information is available free of charge on the ACS Publications website at DOI: 10.1021/acs.joc.6b01904.

Full Gaussian citation, selectivity effects of hydrogen bonds to solvent, alternate reaction pathways, possible mechanism for **B1M** reprotonation, raw data from all tables, and computed geometries, total and free energies, and lowest vibrational frequencies of all species (PDF)

## AUTHOR INFORMATION

### Corresponding Author

\*E-mail: b.janesko@tcu.edu.

### Present Address

<sup>§</sup>Department of Chemistry and Biochemistry, Georgia Institute of Technology, Atlanta, GA, USA.

### Notes

The authors declare no competing financial interest.

## ACKNOWLEDGMENTS

B.G.J. was supported by funds from Texas Christian University. The authors acknowledge the TCU High Performance Computing Center for providing HPC resources.

## REFERENCES

- Yao, T.; Larock, R. C. *J. Org. Chem.* **2005**, *70*, 1432–1437.
- Dong, J.; Wang, F.; You, J. *Org. Lett.* **2014**, *16*, 2884–2887.
- Kundu, N. G.; Khan, M. W. *Tetrahedron* **2000**, *56*, 4777–4792.
- Vasilevsky, S. F.; Mikhailovskaya, T. F.; Mamatyuk, V. I.; Salmikov, G. E.; Bogdanchikov, G. A.; Manoharan, M.; Alabugin, I. V. *J. Org. Chem.* **2009**, *74*, 8106–8117.
- Bubar, A.; Estey, P.; Lawson, W.; Eisler, S. J. *Org. Chem.* **2012**, *77*, 1572–1578.
- Li, D. Y.; Shi, K. J.; Mao, X. F.; Zhao, Z. L.; Wu, X. Y.; Liu, P. N. *Tetrahedron* **2014**, *70*, 7022–7031.
- Li, L.; Wang, M.; Zhang, X.; Jiang, Y.; Ma, D. *Org. Lett.* **2009**, *11*, 1309–1312.
- (a) Pan, J.; Xu, Z.; Zeng, R.; Zou, J. *Chin. J. Chem.* **2013**, *31*, 1022–1026. (b) Zhang, L.; Zhang, Y.; Wang, X.; Shen, J. *Molecules* **2013**, *18*, 654–665.
- Jithunsa, M.; Ueda, M.; Miyata, O. *Org. Lett.* **2011**, *13*, 518–521.
- Long, Y.; She, Z.; Liu, X.; Chen, Yu. *J. Org. Chem.* **2013**, *78*, 2579–2588.
- (a) Zhang, S.-L.; Liu, L.; Fu, Y.; Guo, Q.-X. *Organometallics* **2007**, *26*, 4546–4554. (b) Jones, G. O.; Liu, P.; Houk, K. N.; Buchwald, S. L. *J. Am. Chem. Soc.* **2010**, *132*, 6205–6213. (c) Zou, L.-H.; Johansson, A.; Zuidema, E.; Bolm, C. *Chem. - Eur. J.* **2013**, *19*, 8144–8152. (d) Shi, W.; Liu, W.; Lei, A. *Chem. Soc. Rev.* **2011**, *40*, 2761–2776.
- (a) Becke, A. D. *J. Chem. Phys.* **1993**, *98*, 5648–5652. (b) Becke, A. D. *Phys. Rev. A: At., Mol., Opt. Phys.* **1988**, *38*, 3098–3100. (c) Frisch, M. J. et al. *Gaussian 09*, Revision B.01; Gaussian, Inc.: Wallingford, CT, 2010. (d) Hehre, W. J.; Stewart, R. F.; Pople, J. A. *J. Chem. Phys.* **1969**, *51*, 2657. (e) Krishnan, R.; Binkley, J. S.; Seeger, R.;

Pople, J. A. *J. Chem. Phys.* **1980**, *72*, 650. (f) Perdew, J. P. *Electronic structure of solids '91*; Akademie Verlag: Berlin, 1991; pp 11–20.

(13) Klamt, A.; Jonas, V.; Burger, T.; Lohrenz, J. C. W. *J. Phys. Chem. A* **1998**, *102*, 5074.

(14) Hay, P. J.; Wadt, W. R. *J. Chem. Phys.* **1985**, *82*, 270–283.

(15) (a) Kim, Y.; Mohrig, J. R.; Truhlar, D. G. *J. Am. Chem. Soc.* **2010**, *132*, 11071. (b) . (c) Ribeiro, R. F.; Marenich, A. V.; Cramer, C. J.; Truhlar, D. G. *J. Phys. Chem. B* **2011**, *115*, 14556.

(16) (a) Sham, Y. Y.; Chu, Z. T.; Warshel, A. J. *J. Phys. Chem. B* **1997**, *101*, 4458–4472. (b) Ho, J. M.; Coote, M. L. *WIREs Comp. Mol. Sci.* **2011**, *1*, 649–660.

(17) Bordwell, F. G. *Acc. Chem. Res.* **1988**, *21*, 456–463.

(18) Strieter, E. R.; Blackmond, D. G.; Buchwald, S. L. *J. Am. Chem. Soc.* **2005**, *127*, 4120.

(19) Chinchilla, R.; Najera, C. *Chem. Soc. Rev.* **2011**, *40*, 5084–5121.

(20) Warshel, A. *Computer Modeling of Chemical Reactions in Enzymes and Solutions*; Wiley: New York, 1997.